

Supporting Information for

Improved Separate Solution Method for Determination of Low Selectivity Coefficients

Vladimir V. Egorov[†], Elena A. Zdrachek[‡], and Valentine A. Nazarov[‡]

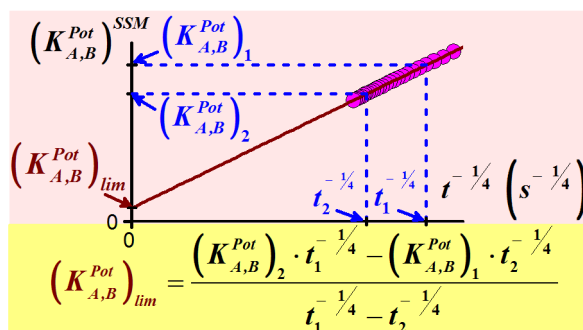
[†]Department of Analytical Chemistry, Belarusian State University,

Leningradskaya str., 14, 220030 Minsk, Belarus

[‡]Research Institute for Physical Chemical Problems of the Belarusian State University,

Leningradskaya str., 14, 220030 Minsk, Belarus

ABSTRACT. Simple, fast and theoretically substantiated experimental method for determination of improved selectivity coefficients is proposed. The method is based on the well-known fact that low selectivity coefficients determined by separate solution method (SSM) are time-dependent and on our finding that this dependence is a well-defined linear function of time raised to the certain negative power. In particular, the selectivity coefficients obtained for equally charged primary and foreign ions by SSM linearly depend on time to the minus one fourth. It was found that extrapolation of experimental data using this function to the intersection with Y-axis gives reliable values of rather low selectivity coefficients (down to $n \times 10^{-7}$) which strongly differ from those measured using SSM and correspond well with the values obtained using the modified separate solution method (MSSM) proposed by Bakker. At the same time the new method is free of one very essential limitation inherent to MSSM, namely it is applicable after the conditioning of electrodes in the primary ion solution and can be repeated many times.



Experimental details.

Reagents. Potassium *tetrakis*(4-chlorophenyl)borate (KTpClPB), tridodecylmethylammonium chloride (TDDMA Cl), dibenzo-18-crown-6 (DB-18-C-6), *tris*(2-ethylhexyl)phosphate (TEHP), 2-nitrophenyl octyl ether (NPOE) and high molecular weight poly(vinyl)chloride (PVC) were of Selectophore grade (Fluka, Buchs, Switzerland). Tetrabutylammonium bromide (Bu₄NBr) (Fluka, Buchs, Switzerland), tetraethylammonium bromide (Alfa Aesar, Karlsruhe, Germany) and triethylammonium chloride (Sigma-Aldrich, Taufkirchen, Germany) were of puriss grade. Rimantadine hydrochloride (RimHCl) substance (see Figure S1) was obtained from Republic Unitary Enterprise “Center for expertise and testing in health care” (Minsk, Belarus). Sodium chloride (NaCl), sodium bromide (NaBr), sodium fluoride (NaF), sodium benzenesulphonate (C₆H₅SO₃Na), potassium nitrate (KNO₃) and potassium chloride (KCl) were purchased from Reakhim (Moscow, Russia) in puriss grade. Tetrahydrofuran (THF) was from Vekton (St. Petersburg, Russia) in certified grade. 1.0×10^{-1} M sodium picrate (NaPic) solution has been prepared by dissolving picric acid (Reakhim, Moscow, Russia) in the solution of 1.0×10^{-1} M sodium hydroxide (Sigma-Aldrich, Steinheim, Germany) with simultaneous potentiometric pH control.

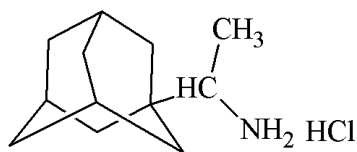


Figure S-1. Chemical structure of Rimantadine hydrochloride

Membrane and Electrode preparation. The membrane cocktails were prepared by dissolving PVC, plasticizer and appropriate amounts of ion exchanger and ionophore in the freshly distilled THF. If the amounts of the ion exchanger or ionophore were very small to weigh precisely, their solutions in THF were made and a calculated aliquot was introduced into the membrane cocktail. After 1 – 2 h of stirring the cocktails were poured into the glass ring fixed on the glass plate. THF was allowed to

evaporate overnight to yield parent membranes of 0.5 – 0.6 mm thickness. Disks of 8 mm diameter were cut from the parent membranes and glued to the PVC tubes with a THF/PVC composition.

EMF Measurements. All measurements were carried out at $20 \pm 1^\circ\text{C}$ using 8-channel pH-meter-ionometer Ecotest-120 (from Econix, Moscow, Russia) combined with PC that allows recording EMF value each 19.7 s automatically. Saturated Ag/AgCl electrode EVL-1M3.1 was used as the outer reference electrode (from Izmeritel, Gomel, Belarus) for all ion-selective electrodes except for RimH^+ -selective electrode. To avoid the influence of KCl leaking from the saturated Ag/AgCl electrode on the potential of RimH^+ -selective electrode LaF_3 F^- -selective electrode (from Econix, Moscow, Russia) was used as the outer reference electrode and 10^{-4} M F^- background was introduced in all sample solutions.

The selectivity behaviour of Bu_4N^+ -selective electrode (10^{-2} mol/kg (0.5 wt %) KTpClPB, 33.0 wt % PVC and 66.5 wt % TEHF), RimH^+ -selective electrode (10^{-2} mol/kg (0.5 wt %) KTpClPB, 5×10^{-2} mol/kg (1.8 wt %) DB-18-K-6, 33.1 wt % PVC and 64.6 wt % TEHF) and Pic^- -selective electrode (10^{-2} mol/kg (0.5 wt %) TDDMA Cl, 32.9 wt % PVC and 66.6 wt % NPOE) has been studied. Unbiased selectivity coefficient values were found by modified separate solution method.¹ The electrodes were conditioned overnight in the foreign ion solutions (1.0×10^{-1} M NaCl in case of Bu_4N^+ -selective electrode, 1.0 M NaCl in case of RimH^+ -selective electrode and 1.0×10^{-1} M NaBr in case of Pic^- -selective electrode) and then the inner reference solutions were introduced (1.0×10^{-1} M NaCl in case of Bu_4N^+ -selective electrode, 1.0×10^{-2} M NaCl in case of RimH^+ -selective electrode and 1.0×10^{-1} M NaBr in case of Pic^- -selective electrode). After that EMF values in different ions solutions were measured in the order of increasing preference. For each interfering ion, the EMF was determined at two concentrations (1.0×10^{-2} and 1.0×10^{-1} M or 1.0×10^{-3} and 1.0×10^{-2} M). The experimental slopes were close to Nernstian in all cases.

For SSM measurements the electrodes with the same membrane compositions were conditioned overnight in the primary ion solution (1.0×10^{-2} M Bu_4NBr , 1.0×10^{-3} M RimHCl or 1.0×10^{-2} M NaPic respectively). The primary ion solution (1.0×10^{-3} M Bu_4NBr , 1.0×10^{-3} M RimHCl or mixture

of 1.8 ml 1.0×10^{-3} M NaPic and 0.5 ml 1.0×10^{-1} M NaCl correspondingly) was introduced as the inner reference solution. The EMF values of the cell containing interfering ion were recorded each 19.7 s during 30 min.

Some $\left(K_{A,B}^{Pot}\right)^{SSM}$ values at chosen time instants are presented in Table S1 and the corresponding $\left(K_{A,B}^{Pot}\right)^{SSM} - t^{-1/4}$ functions are shown in Figures S2 – S8. One can see that the electrode response slopes in all foreign ion solutions except for Br^- solutions are close to the half-Nernstian one (in case of Br^- ions the $\left(K_{A,B}^{Pot}\right)_{lim}$ value has been estimated only for 1.0 M solution). So $\left(K_{A,B}^{Pot}\right)^{SSM}$ values strongly depend on the foreign ion concentration as to be expected. Besides $\left(K_{A,B}^{Pot}\right)^{SSM}$ values strongly depend on the measurement time and are far from the unbiased $\left(K_{A,B}^{Pot}\right)_{Bakker}$ values even in case when discrimination is not very high, e.g. for the pair Bu_4N^+ and Et_3NH^+ . On the contrary, the utmost $\left(K_{A,B}^{Pot}\right)_{lim}$ values (see Figures S2 – S8) estimated as linear regression intercepts for different concentrations of foreign ions coincide well and are close to the unbiased values.

Table S-1. $\left(K_{A,B}^{Pot}\right)^{SSM}$ values measured at different time instants for Pic^- -SE and Bu_4N^+ -SE.

Ions A, B	c_B, M	$\theta_{5.26 \text{ min}},$ mV/decade	$\log\left(K_{A,B}^{Pot}\right)_{Bakker}$ n=3, P=0.95	$\log\left(K_{A,B}^{Pot}\right)^{SSM}$			
				2.30 min	5.26 min	10.20 min	30.25 min
$\text{Pic}^-, \text{Br}^-$	1.0×10^{-1}	-17.6	-6.47 ± 0.02	-	-	-	-
	1.0			-5.42	-5.50	-5.57	-5.67
$\text{Pic}^-, \text{NO}_3^-$	1.0×10^{-2}	-22.5	-5.49 ± 0.03	-3.92	-4.00	-4.06	-4.12
	1.0×10^{-1}			-4.47	-4.54	-4.60	-4.67

Pic ⁻ , C ₆ H ₅ SO ₃ ⁻	1.0 × 10 ⁻²	-22.5	-5.46 ± 0.03	-3.81	-3.90	-3.97	-4.04
	1.0 × 10 ⁻¹			-4.42	-4.49	-4.54	-4.62
Bu ₄ N ⁺ , Na ⁺	1.0 × 10 ⁻²	27.4	-4.52 ± 0.10	-3.47	-3.55	-3.60	-3.69
	1.0 × 10 ⁻¹			-4.00	-4.06	-4.10	-4.18
Bu ₄ N ⁺ , Et ₄ N ⁺	1.0 × 10 ⁻²	29.7	-4.12 ± 0.06	-3.16	-3.23	-3.28	-3.36
	1.0 × 10 ⁻¹			-3.62	-3.68	-3.72	-3.76
Bu ₄ N ⁺ , Et ₃ NH ⁺	1.0 × 10 ⁻³	37.3	-3.33 ± 0.03	-2.45	-2.52	-2.58	-2.64
	1.0 × 10 ⁻²			-2.80	-2.86	-2.91	-2.96

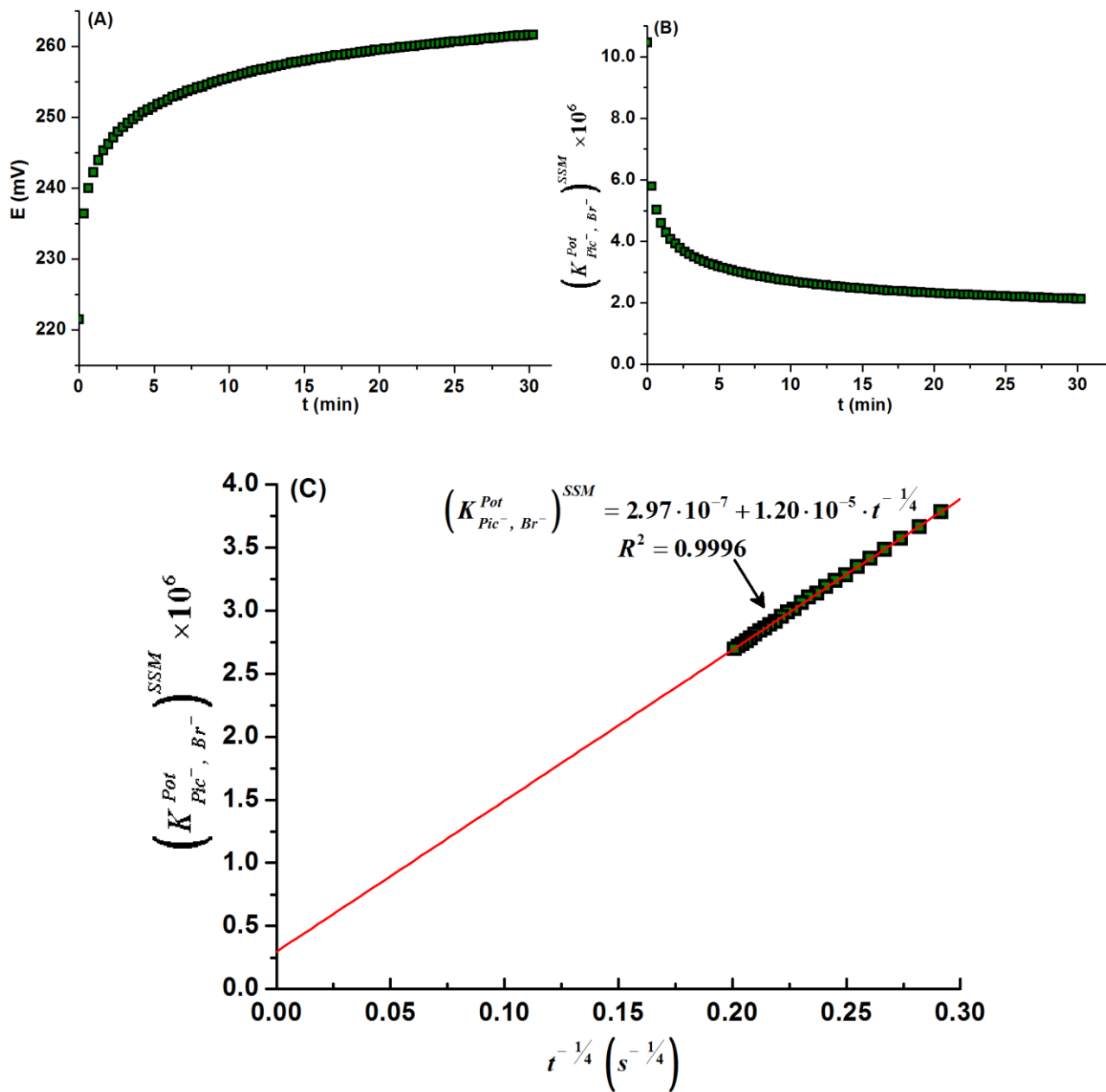


Figure S-2. (A) Electrode potential – time, (B) selectivity coefficient – time and

(C) $(K_{A,B}^{Pot})^{SSM} - t^{-1/4}$ dependencies for Pic^- -SE in 1.0 M Br^- solution.

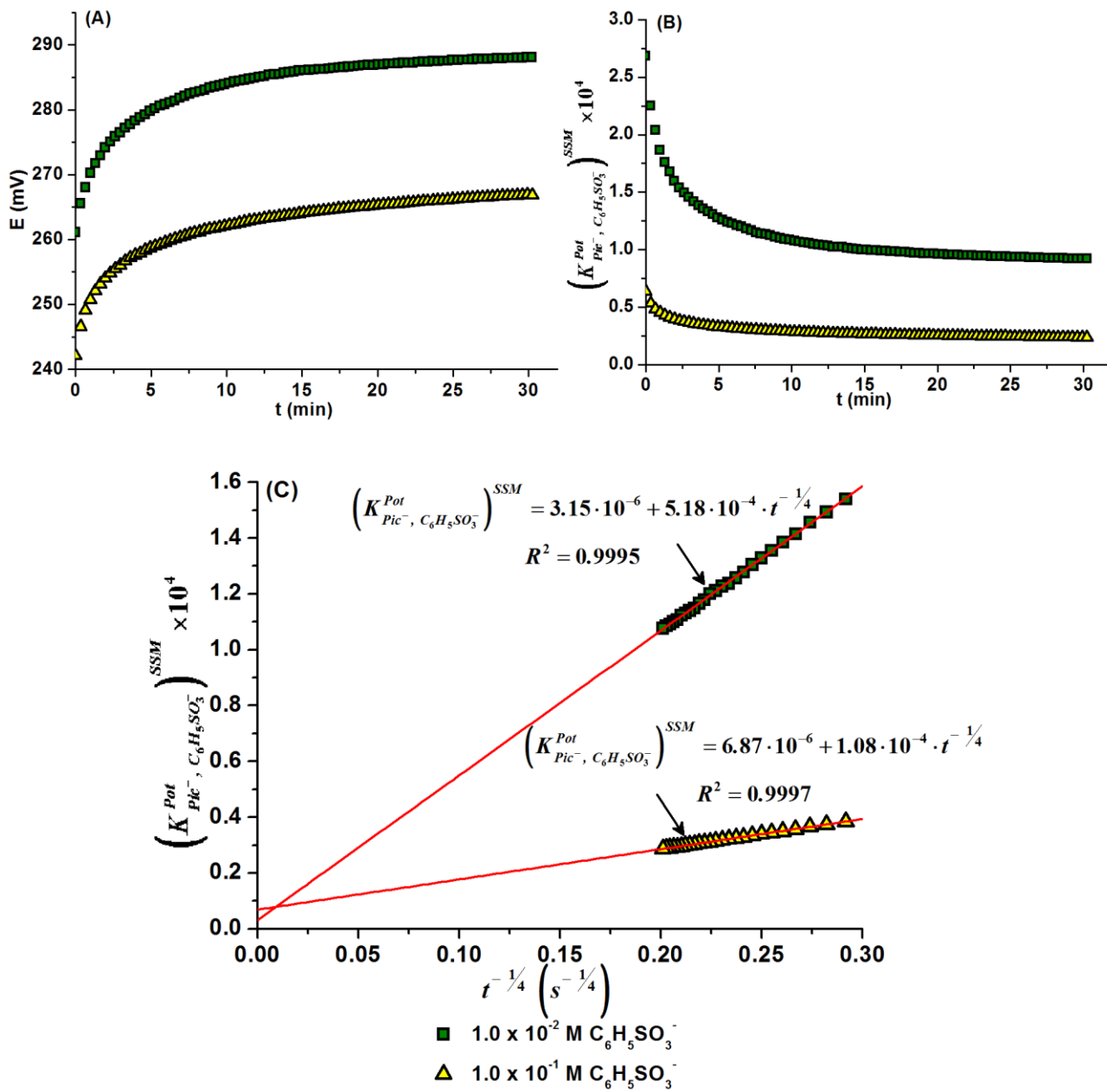


Figure S-3. (A) Electrode potential – time, (B) selectivity coefficient – time and

(C) $\left(K_{A,B}^{Pot}\right)^{SSM} - t^{-1/4}$ dependencies for Pic⁻-SE in $1.0 \times 10^{-2} \text{ M}$ and $1.0 \times 10^{-1} \text{ M } C_6H_5SO_3^-$ solutions.

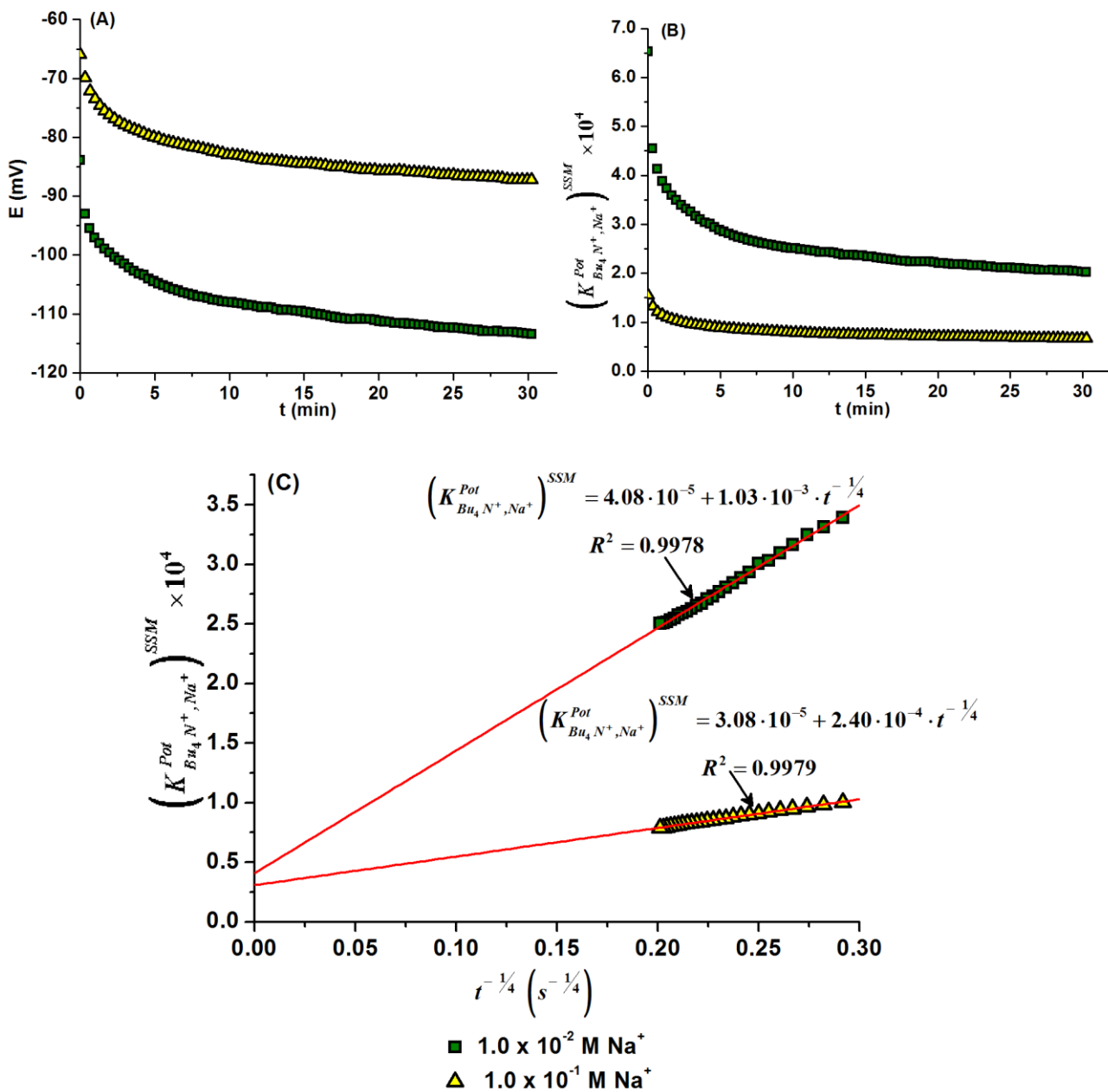


Figure S-4. (A) Electrode potential – time, (B) selectivity coefficient – time and

(C) $\left(K_{A,B}^{\text{Pot}}\right)^{\text{SSM}} - t^{-1/4}$ dependencies for Bu_4N^+ -SE 1.0×10^{-2} M and 1.0×10^{-1} M Na^+ solutions.

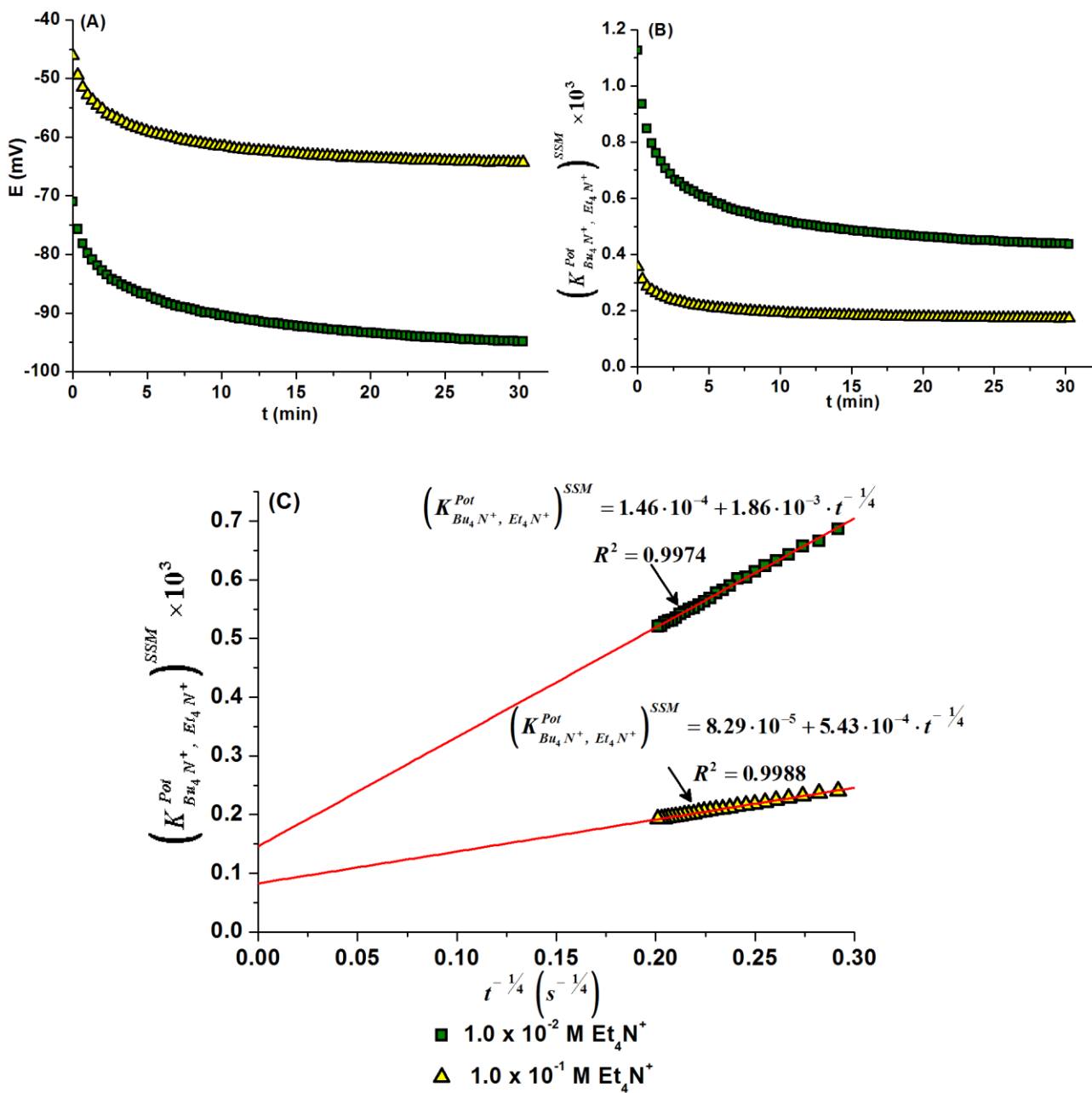


Figure S-5. (A) Electrode potential – time, (B) selectivity coefficient – time and

(C) $\left(K_{A,B}^{Pot}\right)^{SSM} - t^{-1/4}$ dependencies for Bu_4N^+ -SE in $1.0 \times 10^{-2} \text{ M}$ and $1.0 \times 10^{-1} \text{ M Et}_4\text{N}^+$ solutions.

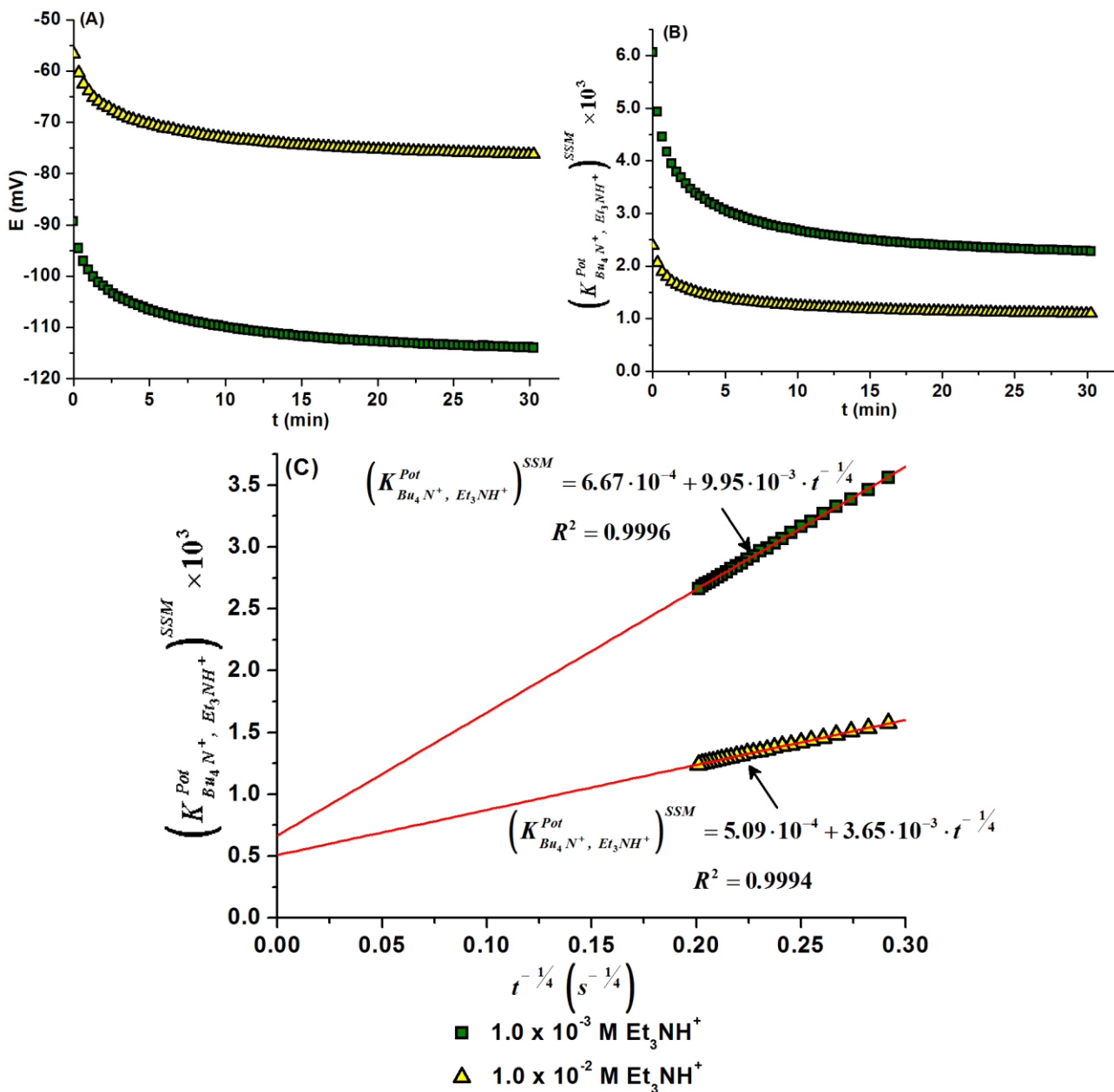


Figure S-6. (A) Electrode potential – time, (B) selectivity coefficient – time and

(C) $\left(K_{A,B}^{\text{Pot}}\right)^{\text{SSM}} - t^{-1/4}$ dependencies for Bu_4N^+ -SE in $1.0 \times 10^{-3} \text{ M}$ and $1.0 \times 10^{-2} \text{ M Et}_3\text{NH}^+$ solutions.

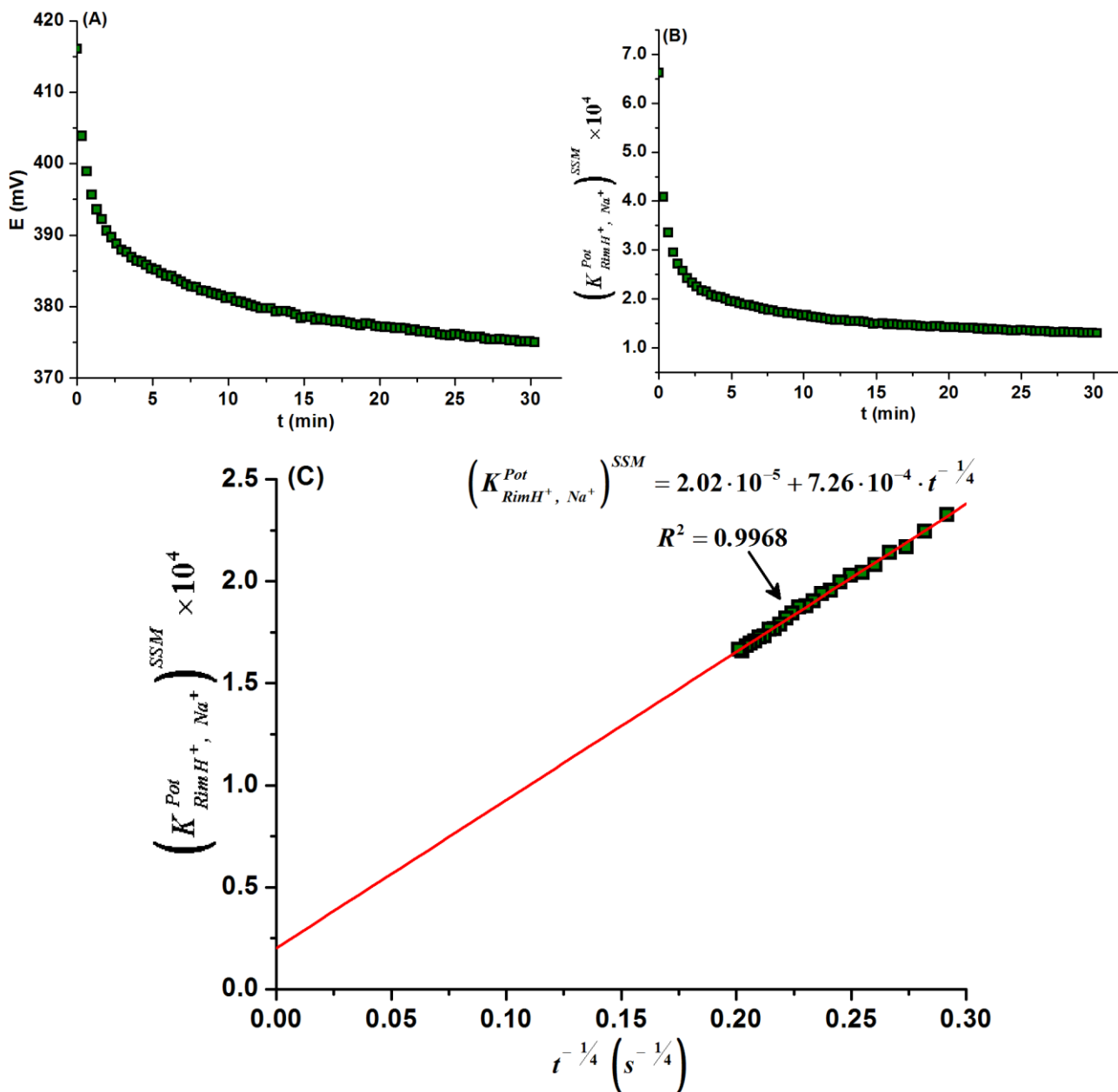


Figure S-7. (A) Electrode potential – time, (B) selectivity coefficient – time and (C) $(K_{A,B}^{Pot})^{SSM} - t^{-1/4}$ dependencies for RimH⁺-SE in 1.0×10^{-2} M Na⁺ solutions.

$$\left((K_{RimH^+, Na^+}^{Pot})_{Bakker} \right) = 2.1 \times 10^{-5}$$

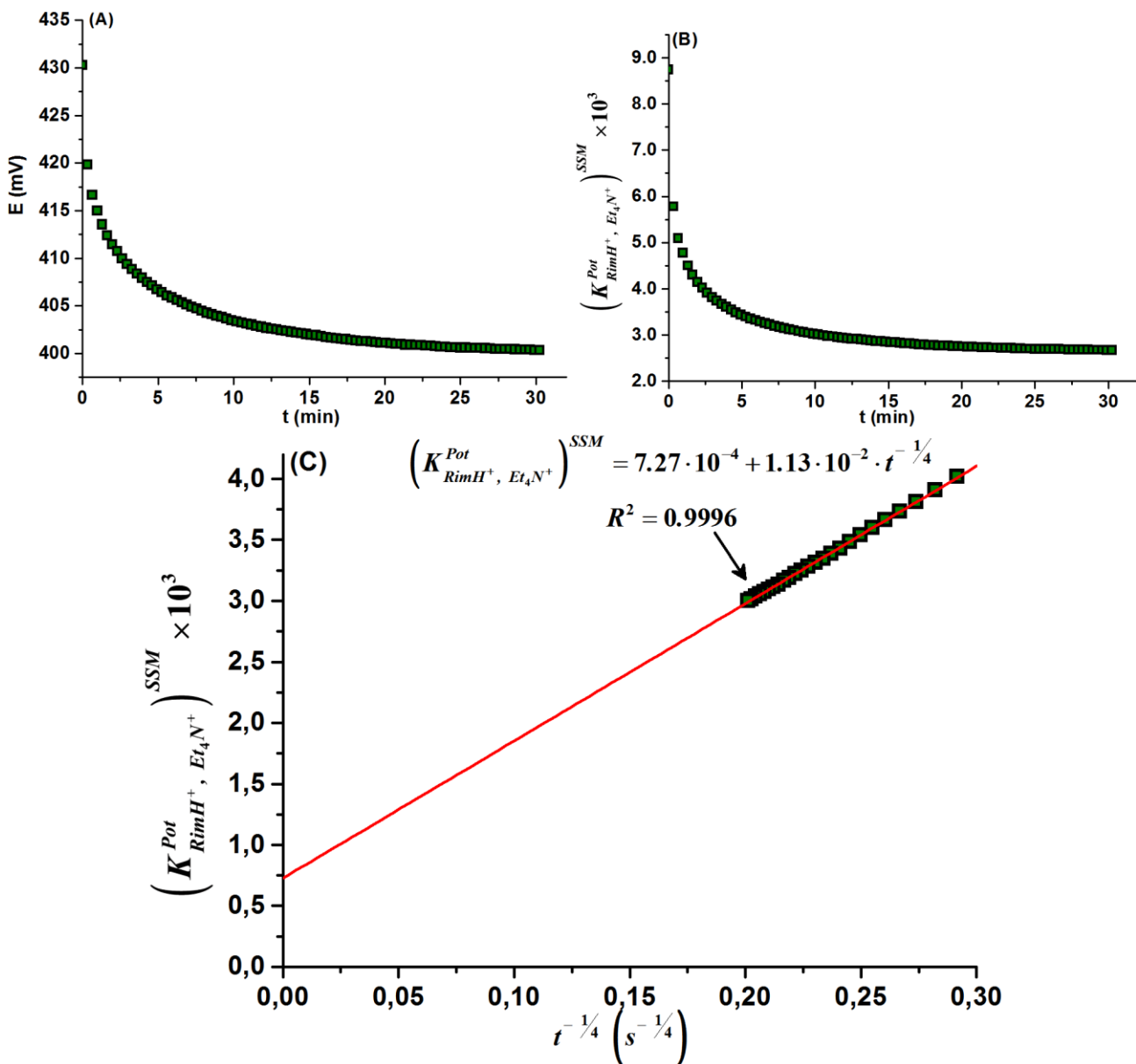


Figure S-8. (A) Electrode potential – time, (B) selectivity coefficient – time and

(C) $\left(K_{A,B}^{Pot}\right)^{SSM} - t^{-1/4}$ dependencies for RimH⁺-SE in 1.0×10^{-3} M Et₄N⁺ solution

$$\left(\left(K_{RimH^+, Et_4N^+}^{Pot}\right)_{Bakker} = 4.9 \times 10^{-4}\right).$$

The examples of deviation of $\left(K_{A,B}^{Pot}\right)^{SSM} - t^{-1/4}$ dependencies from the linearity are presented in

Figure S-9. This deviation can be caused by two main reasons. First, decrease of the primary ion

concentration $\overline{c'_A}$ in the surface membrane layer. In fact, $\overline{c'_B} = \frac{a'_A}{q}$. At the first approximation,

$a'_A = f\left(t^{-1/4}\right)$, while $q = f\left(t^{-1/2}\right)$. So, $\overline{c'_B}$ should grow with time increase and, according to the

material balance equation $\overline{c'_A} = \overline{c_R^{tot}} - \overline{c'_B}$, $\overline{c'_A}$ should decrease with time increase. As a result the equation

(5) is valid if the measuring time is not too long. And the second reason, the more the measuring time is,

the more interference of the salt bridge electrolyte leaking into the sample solution is.

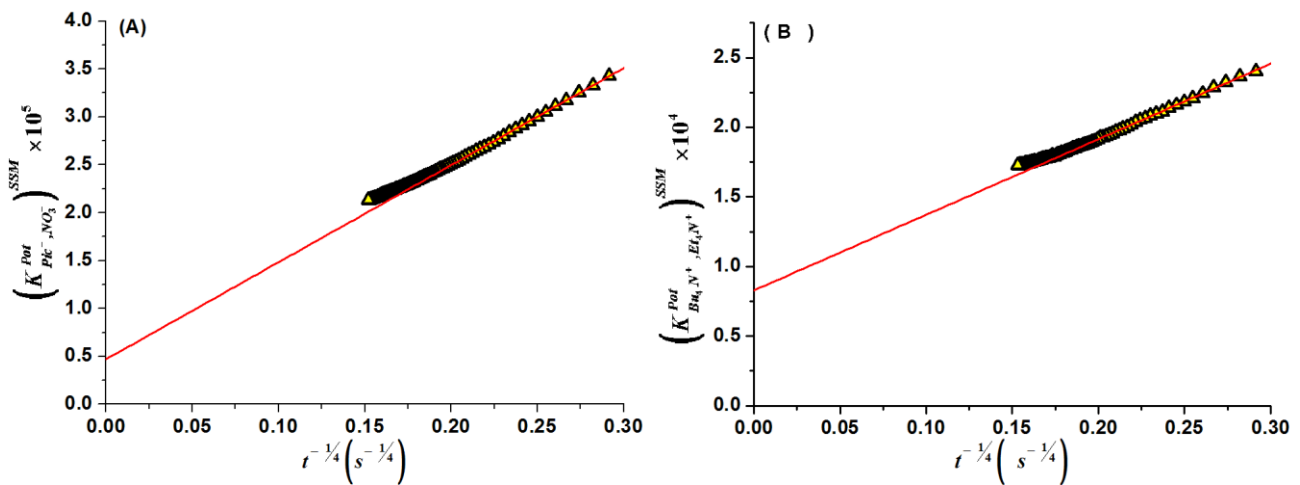


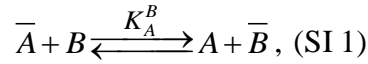
Figure S-9. Deviation of $\left(K_{A,B}^{Pot}\right)^{SSM} - t^{-1/4}$ dependencies from the linearity for Pic^- -SE in

0.1 M NO_3^- solution (A) and for Bu_4N^+ -SE in 0.1 M Et_4N^+ solution (B).

Appendix. Derivation of the equation (4).

Despite of the fact that equation was used to describe the apparent values of the selectivity coefficients², lower detection limits³⁻⁶ we couldn't find its explicit derivation in literature, so it is given below.

If a membrane in form of a primary ion A is immersed into solution of a foreign ion B the ion exchange process takes place at the membrane / solution interface:



where symbols with and without horizontal bars denote the membrane phase and the sample phase respectively, K_A^B is the equilibrium constant.

If the ion exchange equilibrium is fast enough the following equation is valid:

$$K_A^B = \frac{a'_A \cdot \bar{a}'_B}{\bar{a}'_A \cdot a'_B}, \quad (\text{SI } 2)$$

where strokes at the activity symbols denote the activities of the corresponding ions in the surface layers of the membrane or sample solution which differ from the corresponding activities in the bulk of phases.

Due to gradients of activities caused by the ion exchange process the fluxes of the ions in both phases arise. Assuming steady state at any fixed time instant, the rate of ion A delivery from the membrane bulk to the surface is equal to the rate of its withdrawal from the surface to the bulk of the sample solution:

$$\bar{J}_A = \frac{(\bar{a}_A - \bar{a}'_A)\bar{D}_A}{\bar{\delta}_A} = J_A = \frac{(a'_A - a_A)D_A}{\delta_A}, \quad (\text{SI } 3)$$

where \bar{J}_A, J_A are absolute values of ion A fluxes in the membrane and sample solution phases, \bar{D}_A, D_A and $\bar{\delta}_A, \delta_A$ are corresponding diffusion coefficients and thicknesses of the diffusion layers. In analogous,

$$\bar{J}_B = \frac{(\bar{a}'_B - \bar{a}_B)\bar{D}_B}{\bar{\delta}_B} = J_B = \frac{(a_B - a'_B)D_B}{\delta_B}, \quad (\text{SI } 4)$$

Besides, according to ion exchange process the rate of delivery of ion A from the membrane bulk to the interface and the rate of delivery of ion B from the bulk of the sample solution to the interface should correspond to each other:

$$\bar{J}_A = J_B \quad (\text{SI } 5)$$

Taking into account equations (SI 3) and (SI 4) the following equality is valid:

$$\frac{(a'_A - a_A)D_A}{\delta_A} = \frac{(\overline{a'_B} - \overline{a_B})\overline{D_B}}{\overline{\delta_B}} \quad (\text{SI 6})$$

As far as the sample solution initially does not contain ions A , while the membrane initially does not contain ions B , $a_A = 0$, $\overline{a_B} = 0$. So denoting the diffusion coefficients and thicknesses of the diffusion layers in water and membrane phases as $\overline{D}, D, \overline{\delta}, \delta$ we obtain:

$$\overline{a'_B} = \frac{a'_A}{q}, \quad (\text{SI 7})$$

$$\text{where } q = \frac{\overline{D} \cdot \delta}{D \cdot \overline{\delta}} \quad (\text{SI 8}).$$

Insertion of (SI 7) into (SI 2) gives:

$$a'_A = \left(K_A^B \cdot \overline{a'_A} \cdot a'_B \cdot q \right)^{1/2} \quad (\text{SI 9})$$

Taking into account that for highly selective electrodes considered here the ion exchange equilibrium is strongly shifted to the left, alteration of the ion A activity in the surface layer of the membrane in comparison with its activity in the bulk of the membrane can be neglected ($\overline{a'_A} = \overline{a_A}$). For the same reason: $a'_B = a_B$. And finally, using the concentration for the ion A in the membrane phase instead of its activity, we obtain:

$$a'_A = \left(K_A^B \cdot \overline{c_R^{tot}} \cdot a_B \cdot q \right)^{1/2}, \quad (\text{SI 10})$$

where $\overline{c_R^{tot}}$ is the total concentration of the ion exchanger in the membrane.

Actually the thickness of the diffusion layer in the membrane phase depends on time, so diffusion fluxes are time-dependent as well and we deal with pseudo steady state condition. Alteration of the concentration profiles of the ions in the boundary layers of the membrane and sample solution is illustrated by the Figure S-10.

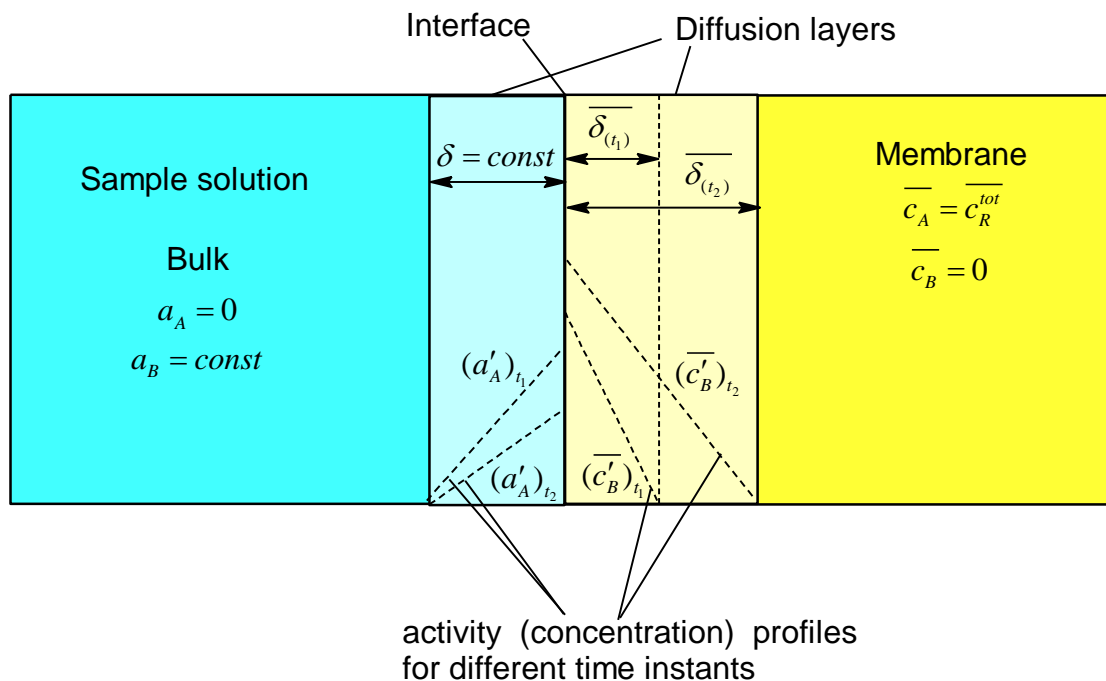


Figure S-10. Schematic representation of the activity (concentration) profiles for the primary ion A in the diffusion layer of the sample solution and for the foreign ion B in the diffusion layer of the membrane respectively for different time instants.

$$t_2 = 4t_1; \overline{\delta}_{(t_2)} = 2\overline{\delta}_{(t_1)}; (a'_A)_{t_1} = \sqrt{2}(a'_A)_{t_2}; (\overline{c'_B})_{t_2} = \sqrt{2}(\overline{c'_B})_{t_1}$$

References

- (1) Bakker, E. *Anal. Chem.* **1997**, 69, 1061.
- (2) Morf, W. E. *The principles of ion-selective electrodes and of membrane transport*; Elsevier: New York, 1981.
- (3) Sokalski, T.; Zwickl, T.; Bakker, E.; Pretsch E. *Anal. Chem.* **1999**, 71, 1204.
- (4) Ion, A.C.; Bakker, E.; Pretsch, E. *Anal.Chim.Acta*, **2001**, 440, 71.
- (5) Ceresa, A.; Radu, A.; Peper, S.; Bakker, E.; Pretsch E. *Anal. Chem.* **2002**, 74, 4027.
- (6) Bakker, E., Bühlmann P.; Pretsch E. *Talanta*. **2004**, 63, 3.